18th International Conference on Structural Mechanics in Reactor Technology (SMiRT 18)
Beijing, China, August 7-12, 2005
SMiRT18-F04-7

FORMATION OF STRESS / STRAIN CYCLES FOR ANALYTICAL ASSESSMENT OF FATIGUE CRACK INITIATION AND GROWTH

Alexander Vasilievich TASHKINOV
Engineering Center of Nuclear Equipment Strength (ENES)
P.O.Box 788, Glavpochtamt, Moscow,101000, Russia
Phone: (+7-095)263-7449, Fax: (+7-095)264-7934
E-mail: tashkin@nikiet.ru

ABSTRACT

This paper discusses standard techniques for setting up cycles of stresses, strains and stress intensity factors (SIF) for use in analysing the fatigue characteristics of crack-free components or the fatigue crack growth if crack-like flaws are present. A number of improved techniques are proposed.

An enhanced procedure for analytical description of true metal stress-strain curves, covering plastic effects, is presented. This procedure involves standard physical and mechanical properties of the metal in question, such as ultimate stress, yield stress and elasticity modulus.

It is emphasized that the currently practiced rain-flow method of design cycle formation, which is effective for an actual (truly known) cyclic loading history, is not suitable for a projected (anticipated) history, as it leaves out of account possible variations in the sequence of operating conditions.

Improved techniques for establishing design stress/strain and SIF cycles are described, which make allowance for the most unfavourable sequence of events in the projected loading history.

The paper points to a basic difference in the methods of design cycle formation, employed in assessment of the ***current condition*** of a component (with the actual history accounted for) and in estimation of the ***residual lifetime*** or ***life extension*** (for a projected history).

Key words: fatigue, crack growth, stress-strain curve, design cycles.

1. INTRODUCTION

Special procedures for setting up design cycles of varying stresses and strains in a component area under consideration are used for analysis of the fatigue damage causing crack nucleation in nuclear plant components.

In analysing fatigue-induced growth of the cracks that already exist in a component, a special technique is employed to set up design cycles of variations in the stress intensity factor (SIF) as a characteristic of the stress-strain state at the crack tip.

Given a complicated loading history, the design stress/strain or SIF cycles are usually different from the actual cycles of variations in these characteristics. The reason for this is the fact that the design cycle formation procedures allow for the interdependence of different loading stages in their effect on the rate of fatigue damage cumulation. The approach taken, i.e. whether it is the actual or the projected cyclic loading that is analysed, will also have significant implications. With projected loading, of all the possible cases anticipated the most unfavourable loading sequence, in terms of strength, is accounted for in standard analysis.

This paper discusses the current standard methods for establishing design stress/strain and SIF cycles (including those with allowance for plastic strains), identifies problems in their application, and puts forward a number of improved approaches.

2. FORMATION OF STRESS / STRAIN CYCLES

2.1. Allowance for plastic strains

With high stresses, it is necessary to take into consideration the arising plastic strains (creep effects are not discussed in this paper), which calls for a true stress-strain curve, σ_t - ε_t, of the component material. The only possible exceptions are very approximate methods of elastic-plastic analysis (e.g., ASME, 2001, Sec.III, Div. 1, It. NB-3228.5), which will not be discussed here.

The stress-strain curve does not belong to standard physical and mechanical characteristics of materials. The regulatory documents that prescribe methods for demonstrating the strength of NPP components have special ways to describe it. Thus, in RCC-MR (2002) true stress-strain curves are given in a generic form for sets of steels and temperatures.

Russian Regulations (1989) and Guidelines RD EO 0330-01 (2004) cover components fabricated from steel of more than 100 grades, many of which are represented by several semi-finished products, with their properties varying in a broad range of design temperatures. This makes it impossible to give a curve for each case. For this reason, a calculation procedure was adopted to define a true stress-strain curve for each grade of steel represented by a specific semi-finished product at a given temperature. A cyclic curve may be derived from a monotonic tension curve by doubling the elastic portion. Therefore, the procedure amounts basically to correct description of a true monotonic tension curve. The theoretical grounds for this procedure may be found in a book by Makhutov (1981) and are briefly set forth below.

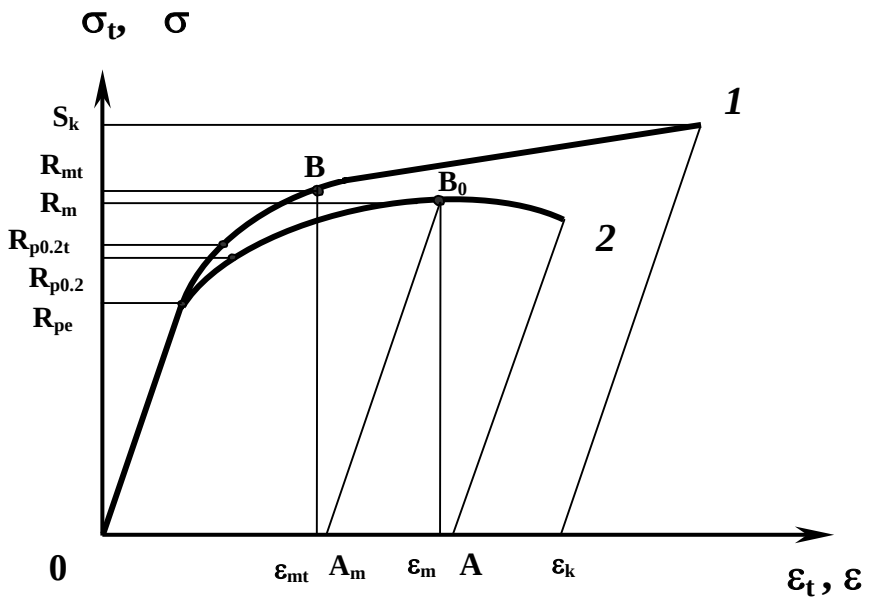

Fig. 1. True (1) and engineering (2) stress-strain curves

In Fig. 1, the true monotonic tension curve is represented by Curve 1 plotted on the σ_t - ε_t coordinates, where σ_t = **P/F** is the ratio of the operating tensile load P to the current cross-section area of the specimen **F**, and ε_t = $\ln(L/L_0)$ is the true or logarithmic strain (**L** – current length of the specimen, and L_0 – its original value).

During standard tensile testing of material specimens, the engineering stress-strain curve is obtained, which is characterized by the elasticity modulus **E**, yield stress $R_{p0.2}$ and ultimate stress R_m. The engineering curve in Fig. 1 appears as Curve 2 with coordinates σ-ε, where $\sigma = P/F_0$ is the ratio of the operating tensile load **P** to the original specimen cross-section area F_0, and $\varepsilon = (L - L_0)/ L_0$ is the conventional strain. The conventional and true strains are related as $\varepsilon = \exp(\varepsilon_t) - 1$. Point B_0 corresponds to the value of $\sigma = R_m$ and identifies the maximum tensile load and the instance of necking initiation. After the specimen unloading from point B_0, the strain corresponds to uniform elongation A_m, and upon the specimen failure, to ultimate elongation **A**.

Strictly speaking, Curves 1 and 2 differ in the values of the proportional limit R_{pe}, as well as in the whole linear portion, but these differences are very small and are disregarded. It is also assumed that $R_{p0.2} \cong R_{p0.2t}$. The difference in the other portions of Curves 1 and 2 is much more significant.

Curve 2 is found experimentally. Curve 1 is calculated using a number of assumptions.

Hooke's law is applied to define the linear portion of Curve 1:

$$\sigma_t = E \cdot \varepsilon_t. \qquad \text{Eq.1}$$

The non-linear portion is treated with regard to the following experimental fact: the non-linear (elastic-plastic) portion of Curve 1 plotted on double logarithmic coordinates, $\log \sigma_t - \log \varepsilon_t$, closely approximates a straight line. This being so, approximation by power function is used for the non-linear portion description:

$$\sigma_t = D \cdot (\varepsilon_t)^{\nu}. \qquad \text{Eq.2}$$

The unknown constants D and ν are determined by the following conditions:

$$\boxed{\text{With } \sigma_t = R_{p0.2} \quad \text{—} \quad \varepsilon_t = R_{p0.2}/E + 0.002} \quad \text{(which follows from determination of } R_{p0.2}\text{)} . \qquad \text{Eq.3}$$

$$\boxed{\text{With } \sigma_t = S_k \quad \text{—} \quad \varepsilon_t = \varepsilon_k = -\ln (1-Z)} \qquad \text{Eq.4}$$

where true resistance to break-off at the neck, S_k, is derived from experimental data as

$$S_k = R_m \cdot (1+1.4 \cdot Z) \qquad \text{Eq.5}$$

with **Z** standing for relative reduction of the specimen cross-section area after the break.

Then, based on the relations of Eqs. 2 – 5, assuming that the material is incompressible and going from natural to decimal logarithms, we arrive at:

$$\nu = \frac{0.73 \cdot \log\left[(1+1.4 \cdot Z) R_m / R_{p0.2}\right]}{\log\left[\dfrac{-2.3 \cdot \log(1-Z)}{2 \cdot 10^{-3} + (R_{p0.2}/E)}\right]} \; ; R_{pe} = \left[\frac{R_{p0.2}}{(2 \cdot 10^{-3} E + R_{p0.2})^{\nu}}\right]^{\frac{1}{1-\nu}} ; \; D = R_{pe}^{\,1-\nu} \cdot E^{\nu}. \qquad \text{Eq.6}$$

The certified values of R_m, $R_{p0.2}$, **Z** and **E** for definition of the true curve are taken from the standards and specifications for materials and semi-finished products, or from the tables of the Regulations (1989).

The above approach (Makhutov, 1981; Regulations, 1989) has been in practical use for decades and has proved very convenient in producing a true curve of material tension with specific values of R_m, $R_{p0.2}$, **Z** and **E** for a temperature under consideration. However, it has significant shortcomings:

1) Equation 2 is assumed to be true for the whole range of plastic deformation to the point of specimen failure. In reality, this is not exactly so. And if we remember that practical strength analyses are performed for relatively low strains (in any case no higher than ε_{mt}, or even lower with regard to the current set of safety factors), then it will be apparently inappropriate to extend the approximation of Eq.2 to the whole range of deformation ending in failure.

2) Equation 5 is experimentally supported only for some low-carbon and low-alloy ductile steels (Makhutov, 1981). Its extension to the whole set of structural steels accepted for use in nuclear engineering is hypothetical.

3) The resulting relations of Eq.6 include quantity **Z**, whose role appears questionable for practical values of strain no higher than ε_{mt}, when the processes of necking and specimen failure are not yet credible.

4) The hypotheses of Eqs. 2 and 5 along with the relations of Eqs.3 and 4 ignore the fact of existence of an extremum at point B_0 of Curve 2 in Fig. 1 at $\sigma = R_m$, which is inconsistent with experimental data.

5) True strains ε_t, unlike conventional strains ε, do not form a tensor field. That is why TRUE stresses and CONVENTIONAL strains are used in classical elasticity and plasticity theories, as well as in practical analyses and their associated software. For elastic-plastic analysis, as part of cyclic strength analysis, the formulae of Eq.6 may also be used for conventional strains, because with deformation as high as 5% there is negligible difference between true and conventional strains. On the other hand, in calculations for high strains (e.g., in limit analyses), the characteristics of σ_t - ε curve rather than ones of Eq.6 formulae are required. (It should be remembered that classification of stresses into true and engineering ones is only relevant for results of tensile tests. It is only true stresses, designated as σ, that are applied in structural analysis.)

To avoid the above shortcomings, the following upgraded approach is proposed for the true curve description. The approximation of Eq.2 will be used as before. To find quantities **D** and **ν**, the relationship in Eq.3 is to be used and the relationship of Eq.4 should be replaced by the condition resulting from determination of R_m:

$$\boxed{\textbf{Given } \sigma = R_m\textbf{, an extremum is reached in the engineering stress-strain curve.}} \qquad \text{Eq.7}$$

It is known that the relationship of Eq.7 is equivalent to the condition that true strain at point **B** is equal to ν. This will be demonstrated below, as presented by Birger & Mavlyutov (1986).

The extremum in the engineering stress-strain curve corresponds to the peak value of the tensile load, $\mathbf{P = \sigma_t \cdot F}$, i.e.:

$$\mathbf{dP = d\sigma_t \cdot F + \sigma_t \cdot dF = 0,} \quad \text{or} \quad \mathbf{d\sigma_t / \sigma_t = -dF/F.} \qquad \text{Eq.8}$$

Assuming retention of the metal volume,

$$\mathbf{d(F \cdot L) = dF \cdot L + F \cdot dL = 0,} \quad \text{or} \quad \mathbf{dL / L = -dF/F.} \qquad \text{Eq.9}$$

From Eqs.8 and 9 it follows that

$$\mathbf{d\sigma_t / \sigma_t = dL/L = d\varepsilon_t.} \qquad \text{Eq.10}$$

For point B_0, corresponding to the extremum in Curve 2,

$$\mathbf{d\sigma_t / d\varepsilon_t = \sigma_t.} \qquad \text{Eq.11}$$

Inclusion of the approximation of Eq.2 leads to the relationship sought:

$$\text{With } \mathbf{\sigma_t = R_{mt}}, \quad \mathbf{\varepsilon_t = \nu.} \qquad \text{Eq.12}$$

Proceeding from Eq.12 and allowing for Eqs.2 and 3, we arrive at

$$\left(\frac{\nu / 2.72}{R_{p0.2} / E + 0.002} \right)^{\nu} = \frac{R_m}{R_{p0.2}}; \qquad \text{Eq.13}$$

$$D = R_m \left(\frac{2.72}{\nu} \right)^{\nu}; \qquad R_{pe} = R_m^{\frac{1}{1-\nu}} \cdot \left(\frac{2.72}{E \cdot \nu} \right)^{\frac{\nu}{1-\nu}}. \qquad \text{Eq.14}$$

In practice, the value of ν may be calculated by solving Eq.13 by the trial-and-error method, or by making use of graphs based on Eq.13. An example of such graphs is given in Fig. 2. Using the value of ν obtained, **D** and $\mathbf{R_{pe}}$ are deduced from relationships of Eqs.14.

The relationships of Eqs.13 and 14 define the non-linear portion of the true stress-strain curve based on the standard **E,** $\mathbf{R_m}$ and $\mathbf{R_{p0,2}}$, without resorting to quantity **Z** (which is important when no **Z** data are available). In this case, an extremum is sure to be found in Curve 2 (Fig. 1) with $\mathbf{\sigma = R_m}$.

Figures 3 and 4 provide comparison of true stress-strain curves constructed from the standard formulae of Eqs.6 and from the proposed formulae of Eqs.13 and 14. These figures show that the difference may be either very significant (as is the case with Russian austenitic stainless steel 08X18H10T) or practically nonexistent (Russian pearlitic alloyed chromium-molybdenum-vanadium steel 15X2HMΦA). Point B in the curves corresponds to $\mathbf{R_{mt}}$ and $\mathbf{\varepsilon_{mt}}$, i.e. to necking initiation.

The proposed method of calculating a true stress-strain curve may also be applied for analytical evaluation of relative uniform elongation $\mathbf{A_m}$, as well as of the ultimate strains $\mathbf{\varepsilon_{mt}}$ and $\mathbf{\varepsilon_m}$, involved in limit analyses, calculations of brittle fracture resistance, etc.

Thus, with ν found from Eq.13, we arrive at:

$$\mathbf{\varepsilon_{mt} = \nu,} \qquad \text{Eq.15}$$

$$\mathbf{\varepsilon_m = \exp(\nu) - 1,} \qquad \text{Eq.16}$$

$$\mathbf{A_m = \exp(\nu) - R_m/E - 1.} \qquad \text{Eq.17}$$

The proposed analytical evaluation of A_m was checked for accuracy by comparison with experimental data. The results presented in Table 1 for a number of Russian steel grades show good agreement.

It should be noted here that point **B** lies in the gently sloping curve portion, which is why minor inaccuracies that may occur in finding its horizontal coordinate (caused by an error in determining $\mathbf{A_m}$) will have little effect on definition of the true stress-strain curve.

As mentioned above, practical elastic-plastic analyses for cases of high strains often call for a stress-strain curve plotted on coordinates of true stresses and conventional strains, $\mathbf{\sigma_t - \varepsilon.}$ To this end, the relationship between the true and conventional strains

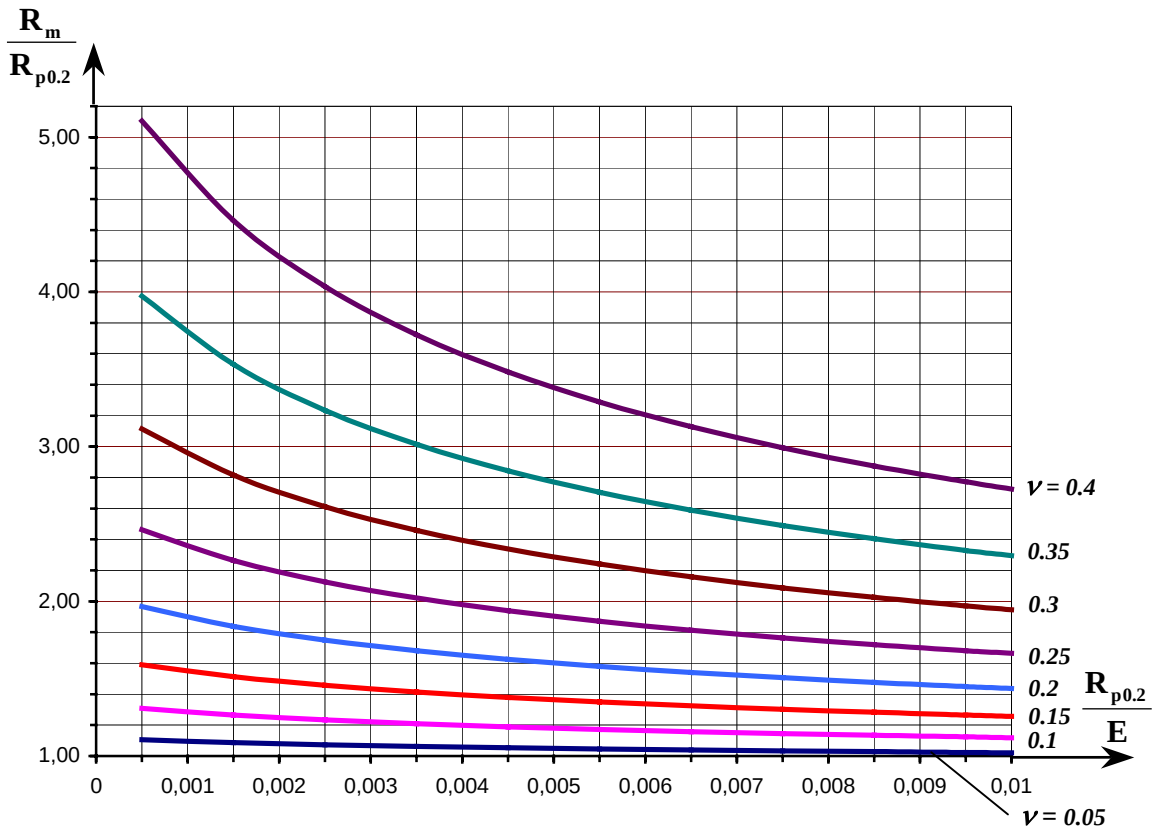

Fig. 2. Graph for evaluation of work hardening parameter ν

$$\varepsilon_t = \ln(\varepsilon + 1) \qquad \text{Eq.18}$$

should be substituted in the approximation of Eq.2. As a result, we find the relationship describing the design stress-strain curve

$$\sigma_t = D\cdot[\ln(\varepsilon + 1)]^{\nu}, \qquad \text{Eq.19}$$

for which parameters **D, ν** and, if required, $\mathbf{R_{pe}}$ are determined from Eqs.13 and 14.

Subsequent discussion will only refer to true stresses, which are designated as **σ**.

2.2. Formation of stress and strain cycles

There is a number of different design cycle formation algorithms described in technical literature. The greatest application has been found by the rain-flow method, which was first proposed by Matsuishi & Endo (1968), and was later developed into a number of modifications and included in some standards. This method provides the most accurate description of the results of many experiments with complicated programmed loading conditions. Thus, it appears best suited for assessing fatigue damage cumulated over an actual loading history.

However, it is not uncommon to see the rain-flow method applied for cases of projected history as well, which may lead to non-conservative results, as shown by Tashkinov (1998).

The regulatory documents specifying design stage calculations set the target at the most hazardous possible combinations of projected loading conditions. Thus, it is required by such documents as the Regulations (1989), and RD EO 0330-01 (2004), that during design calculations for fatigue strength assessment according to crack nucleation criterion, the forthcoming design cycle should be separated from the remains parts of the sequence with the maximum possible stress/strain range. This requirement is associated with the fact that at the design stage it is impossible to predict the consecutive order of actual operating modes, although peak stress/strain values of every mode and scheduled number of their repetition are known beforehand.

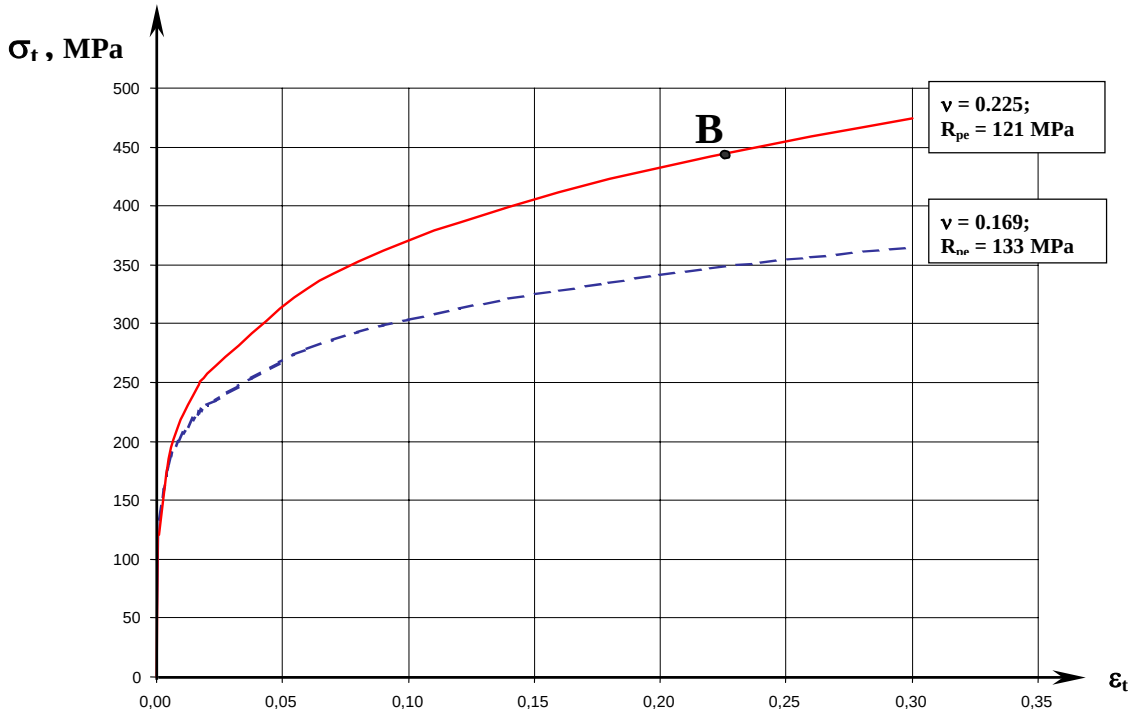

Fig. 3. Comparison of calculated true stress-strain curves for steel 08X18H10T at 350^0C; R_m = 353 MPa, $R_{p0.2}$ = 167 MPa, E = 175 000 MPa:
- - - - – standard approach (Regulations, 1989); ––––– – proposed approach.

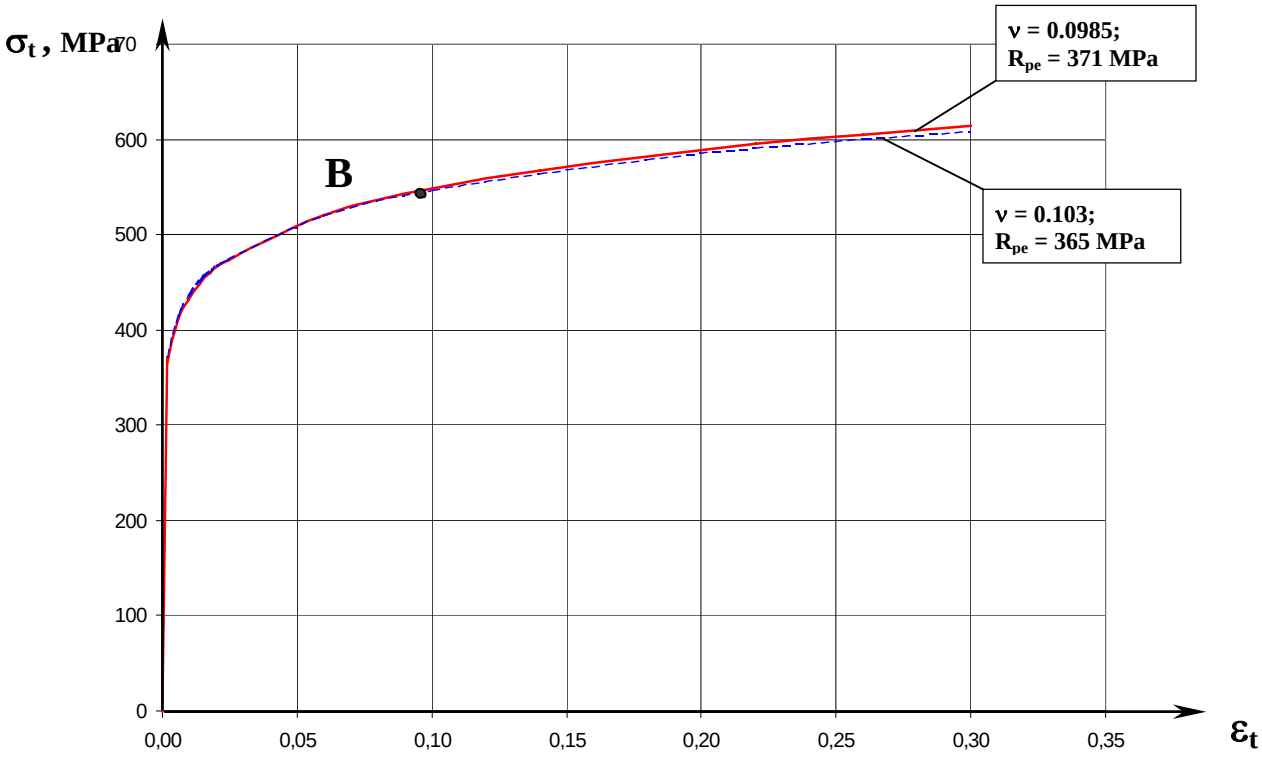

Fig. 4. Comparison of calculated true stress-strain curves for steel 15X2HMΦA at 350^0C; R_m = 491 MPa, $R_{p0.2}$ = 395 MPa, E = 190 000 MPa:
- - - - – standard approach (Regulations, 1989); ––––– – proposed approach.

Table 1. Comparison of calculated and experimental values of A_m

No.	Steel Grade	R_m, MPa	$R_{p0.2}$, MPa	$\varepsilon_{mt} = \nu$, Eq.13	A_m, %		Reference
					Experiment	Eq.17	
1	St 3*)	445	225	0.212	20 19.5 20 20.7	23	Kuzema (1975)
2	St 4	504	270	0.202	20.4	22	Shevandin & Razov (1965)
3	20**)	460	290	0.163	15	17	
4		470	290	0.168	16.5	18	
5	09Г2С*)	505	285	0.190	19.6 19.6 19.1 18.5	21	Kuzema (1975)
6	16Г2С *)	460	270	0.178	21.2 22.5 20 21	19.5	Kuzema (1975)
7	12Х2Н4А*)	695	605	0.08	7.85 7.7 8.4 8.0	8	Kuzema (1975)
8	12ХН3МА	795	716	0.07	6.5	6.9	Shevandin & Razov (1965)
9	15ХН2МА**)	736	646	0.078	10,2	7.8	
10		1080	1030	0.050	6.6	4.6	
11		1190	1170	0.034	4.3	3.0	
12		1260	1240	0.034	4.5	2.9	
13	20Х2Н4А*)	1000	900	0.075	5.1 5.15	7.3	Kuzema (1975)
14	30Х2НМА**)	1030	980	0,05	6,5	4,6	Shevandin & Razov (1965)
15		1150	1120	0.04	6.6	3.5	
16		1290	1260	0.04	4.2	3.5	

Notes: *) Several specimens were tested, and their properties were averaged in calculation.
**) Steel of one grade with various heat treatments.

Of the two key parameters in the stress or strain cycle – the range and the asymmetry factor – the former is treated as dominating in the fatigue damage cumulation. As the cycle range grows, fatigue damage shows a sharp non-linear increase, wherefore by taking up first the cycles with the maximum ranges it is possible to ensure coverage of all possible unfavourable loading combinations in the sequence.

Similar regulatory documents of other countries, such as ASME Code (2001) and French rules RCC-MR (2002), have no such requirement in an explicit form, but their cited examples of appropriate design cycle formation are fully consistent with the maximum range principle.

The rain-flow method omits this principle and, hence, in some cases comes into conflict with the regulatory requirements. This may be illustrated (Tashkinov, 1998) by the example presented in Fig. 5 (a), which was borrowed from item RB 3226.2 of RCC-MR (2002). A similar example may be also found in ASME Code (2001), item NB-3222.4(5). According to both regulatory documents, it is prescribed to count two cycles with a range 2-7 and two cycles with a range 3-6, as shown in Fig. 5 (b), which is fully consistent with the requirement of separating a cycle with the maximum possible range. Not so with the rain-flow method, which yields one cycle with a range 2-7, one cycle with a range 2-3, one cycle with a range 3-6, and one cycle with a range 7-8.

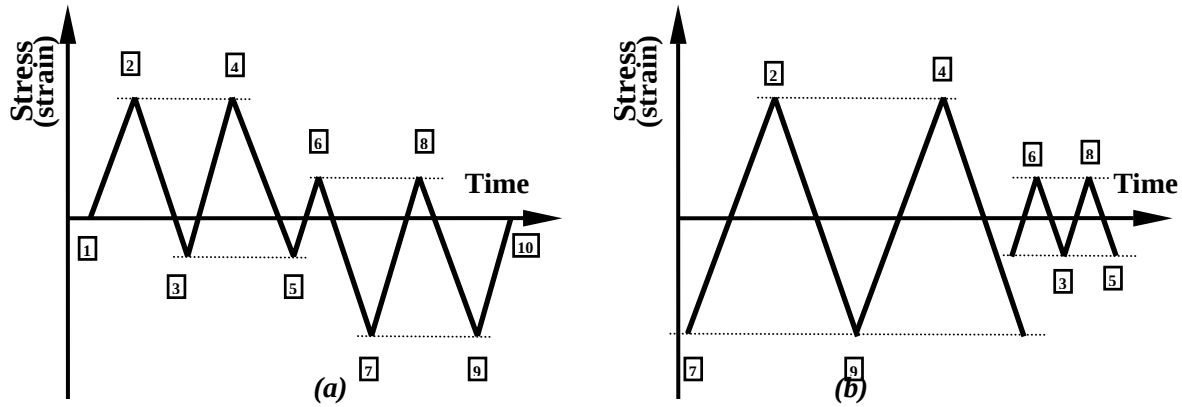

Fig. 5. A regulatory example of design cycle counting (ASME, 2001; RCC-MR, 2002)

A special way to ensure cycle separation by the maximum range principle was proposed by Tashkinov (1998), which is referred to as the shadow method. Its algorithm is easy to implement. Therewith this method rules out formation of unduly conservative cycles, which are physically impossible on account of deformation conditions, as is the case, for instance, with the peak counting method which combines the absolute stress (strain) maximum with the absolute minimum for counted cycles.

The shadow method is briefly described below. The sequence is assumed to be closed, with its starting and end values coinciding. In opposite cases (which usually result from irreversible deformation under plastic conditions), it is advisable to have the sequence artificially closed. The additional conservatism thereby introduced in fatigue damage assessment is not great and may be evaluated, if required.

Consideration is only given either to the ascending or to the descending parts between any adjacent maximum and minimum in the sequence.

The procedure of design cycle counting is the following:

a) The sequence is assumed to be illuminated by a light flux the rays of which directed in parallel to the horizontal time axis. The light is held by these parts. Due to this a vertical shadow spot is formed.

b) The maximum and minimum values of a counted cycle are assumed to be equal to the upper and lower boundaries of the shadow spot, respectively. If two o more spots are produced in the course of one illumination, then a particular counted design cycle corresponds to each of them.

c) After recording a counted cycle (or a number of cycles corresponding to the number of shadow spots in one illumination) the considered parts are transformed: their sections, illuminated by the light flux are deleted from the following considerations. There remains only the sections that were in the shadow.

d) The illumination process ia repeated until all sections of the ascending (descending) parts in question are illuminated.

Figure 6 provides an example of the shadow method applied to the graph of Fig. 5. The separated cycles are shown in the figure as shadow segments. The outcome of the shadow method is fully consistent with the regulatory

design cycles for this example.

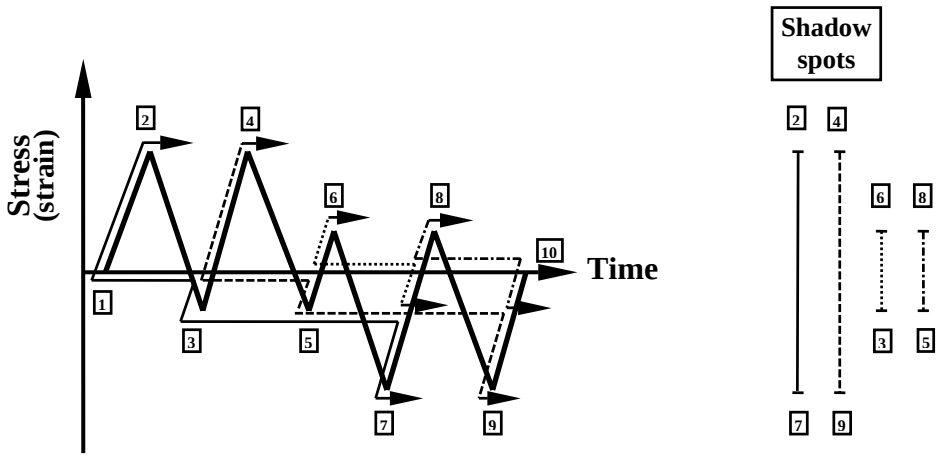

Fig.6. Shadow method as applied to the example of Figure 5:
——— - 1st illumination; — — — - 2nd illumination; ·····– 3rd illumination;
–·–·–·– - 4th illumination.

3. FORMATION OF SIF VARIATION CYCLES

As compared to fatigue damage cumulated before crack nucleation, the task of design cycles formation for a component with a crack is complicated by the fact that the component geometry will change due to the crack growth.

For cases of analytical evaluation of fatigue crack growth under actual loading conditions, the most appropriate approach is to count cycles of SIF variations with the use of the rain-flow method. Extensive experimental studies have been published to support this approach.

On the other hand, prediction of the fatigue crack growth calls for establishing such design cycles that would reliably cover the most unfavourable load combinations among those anticipated.

Regulatory documents address this issue in different ways. In the ASME Code (2001), Sec.XI, Div.1, Apps. A, C, it is recommended to use the chronological sequence of transients specified in the design documentation. The maximum SIF variation range should be considered for each transient. Such an approach is likely to result in non-conservative assessments, as the design-basis sequence is often altered by events that prove unpredictable in advance. Besides, the combined effect of cycles pertaining to different transients on the crack growth rate is left out of account.

Recommendations of the Russian Guidelines RD EO (2004) are based on the requirement of the first priority counting of cycles possessing the maximum possible SIF range throughout the loading history.

The French Rules RCC-M (1988), Sec.1, Subsec. Z, It. ZG 3320, use an approach closely resembling the peak counting method mentioned above: one design cycle combines the absolute maximum with the absolute minimum from the projected SIF variation history. Usually this leads to unduly high conservatism of calculations, but may also prove non-conservative in some cases, as shown below.

A feature shared by regulatory documents is the use of experimental kinetic diagrams, which relate the rate of fatigue crack growth $\mathbf{V = dl/dN}$ (**l** – crack length; **N** – number of cycles) to the range of stress intensity factor variation $\mathbf{\Delta K}$. For their analytical description it is common practice to use relationships of the Paris equation type:

$$\mathbf{dl/dN = C(\Delta K_{ef})^{m} = V} \,. \qquad \text{Eq.20}$$

The effective SIF range over a cycle, $\mathbf{\Delta K_{ef}}$, may account for the effect of the cycle asymmetry, correction for plasticity, crack closure effect, etc. So, in RD EO, (2004) allowance for asymmetry is provided by the following relationship:

$$\mathbf{\Delta K_{ef} = \Delta K / \sqrt{1 - K_{min}/K_{max}}} \qquad \text{Eq.21}$$

where $\mathbf{K_{min}}$ and $\mathbf{K_{max}}$ are the minimum and maximum SIF values in the cycle. In cases when the compressive

part of the SIF variation cycle prevails over the tensile part, use is made of a formula for a symmetric cycle:

$$\Delta K_{ef} = \Delta K / \sqrt{2} . \qquad \text{Eq.22}$$

The results of a study by Tashkinov (1999), which define the rules for formation of design SIF cycles to describe the most hazardous possible load sequence are presented below.

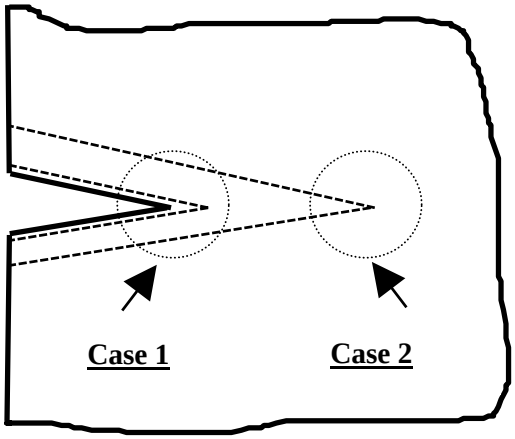

Fig. 7. Limiting cases in crack growth analysis:

- initial crack tip position;
- final crack tip position;
- fatigue damage cumulation zone.

The damage causing fatigue crack growth under cyclic loading, is cumulated in the metal areas at the crack tip, which itself is displaced as the crack grows (see Fig. 7). Consideration is given to the following limiting cases of interaction of various cycle types (with each cycle type characterised by its own system of simultaneously acting loads and by the number of their recurrences):

Case 1. The crack shows little growth over the time taken by the different types of cycles included in the set. It may be assumed that damage is accumulated approximately in one and the same metal area.

Case 2. The crack grows rather quickly, and it may be assumed that the damage caused by cycles of different types is accumulated in different metal areas.

We shall now discuss the ways of establishing the loading histories for these schematic cases, which will help making recommendations for practical analyses.

3.1. Small crack growth (Case 1)

Since the fatigue damage caused by different cycles is accumulated roughly in the same metal area, there will be an interplay between the damage processes resulting from these cycles. This situation is similar to the set-up in analyses of crack-free components for fatigue strength, where the loading history should be established by the principle of the maximum cycle range (see section 2.2).

We are going to demonstrate that this principle is also expedient in the case under consideration.

It is assumed that there are two types of loads variation cycles with the same number of recurrences $\mathbf{N}$ and parameters $\mathbf{K_{1min}}$, $\mathbf{K_{1max}}$, $\mathbf{K_{2min}}$, $\mathbf{K_{2max}}$, with $\mathbf{K_{1min}} < \mathbf{K_{2min}}$. Use of the maximum range principle will be required, if the inequalities $\mathbf{K_{1max}} < \mathbf{K_{2max}}$ и $\mathbf{K_{1max}} > \mathbf{K_{2min}}$ are fulfilled (which is apparent from the graph of stress /strain variations in Fig. 5).

With the fatigue crack growth considered to be fairly small, these two types of cycles may be treated as found in immediate succession in the loading history. This assumption reflects the independence of the resultant small crack growth from the cycle occurrence order.

The maximum range principle should be applied to set up two new types of design cycles with the parameters $\overline{\mathbf{K}}_{\mathbf{1min}} = \mathbf{K_{1min}}$, $\overline{\mathbf{K}}_{\mathbf{1max}} = \mathbf{K_{2max}}$, $\overline{\mathbf{K}}_{\mathbf{2min}} = \mathbf{K_{2min}}$, $\overline{\mathbf{K}}_{\mathbf{2max}} = \mathbf{K_{1max}}$. We shall take $\Delta \mathbf{l}$ to designate the fatigue-induced increment in the crack length as a result of the two initial types of cycles, and $\overline{\Delta \mathbf{l}}$ to stand for the two transformed ones.

In view of the small crack growth, it is believed that the maximum and minimum SIF values remain constant for each cycle type. Then, using the relationships of Eqs.20 and 21, we arrive at:

$$\overline{\Delta \mathbf{l}} - \Delta \mathbf{l} = \mathbf{NC} \cdot [(\mathbf{b}^{m/2} - \mathbf{d}^{m/2}) - (\mathbf{c}^{m/2} - \mathbf{a}^{m/2})] \qquad \text{Eq.23}$$

where $\mathbf{a} = \mathbf{K}_{\mathbf{1max}}^2 - \mathbf{K_{1max}} \cdot \mathbf{K_{2min}}$; $\mathbf{b} = \mathbf{K}_{\mathbf{2max}}^2 - \mathbf{K_{2max}} \cdot \mathbf{K_{1min}}$;

$\mathbf{c} = \mathbf{K}_{\mathbf{1max}}^2 - \mathbf{K_{1max}} \cdot \mathbf{K_{1min}}$; $\mathbf{d} = \mathbf{K}_{\mathbf{2max}}^2 - \mathbf{K_{2max}} \cdot \mathbf{K_{2min}}$.

Given $\mathbf{m = 2}$, it follows from Eq.23 that $\overline{\mathbf{\Delta l}}$ – $\mathbf{\Delta l}$ > 0, as $\mathbf{(b-d)-(c-a) = (K_{2max} - K_{1max}) \cdot (K_{2min} - K_{1min}) > 0}$.

It will be demonstrated that $\overline{\mathbf{\Delta l}}$ – $\mathbf{\Delta l}$ > 0 is also true for $\mathbf{m > 2}$. Considering the nonlinearity of function $\mathbf{y = x^{m/2}}$, as well as the fact that $\mathbf{a < c < b}$, $\mathbf{d > a}$, it may be concluded that with increase in $\mathbf{m}$ the value of $\mathbf{(b^{m/2} - d^{m/2})}$ grows quicker than that of $\mathbf{(c^{m/2} - a^{m/2})}$. In view of Eq.23, this means that $\overline{\mathbf{\Delta l}}$ > $\mathbf{\Delta l}$, i.e. with the design cycles formed by the principle of maximum SIF range, the crack will show the greatest growth.

This situation being similar to the one discussed in section 2.2, it is advisable to use the shadow method for implementing this principle, now applied to the SIF variation history.

3.2. Large crack growth (Case 2)

It is assumed that each cycle of a new type occurs under conditions where the metal at the crack tip is "new" and has practically "no memory" of the damage from the previous cycles of different types. Such a situation is typical for quick crack growth, but it is also possible in cases of small growth (if cycles of different types have such parameters that do not need rearrangement according to the maximum range principle).

Let us determine the order in which cycles of different types should be applied to a component with the initial crack length $\mathbf{l_0}$, to arrive at the greatest possible increase in the crack length $\mathbf{\Delta l}$, which will represent the worst loading sequence among all those possible in reality.

3.2.1. Two successive types of cycles

It is assumed that a component with a crack is subjected to cyclic loading in cycles of two types with the following characteristics: $\mathbf{(\Delta K_{ef})_1}$, $\mathbf{N_1}$, $\mathbf{C_1}$, $\mathbf{m_1}$ and V_1, and $\mathbf{(\Delta K_{ef})_2}$, $\mathbf{N_2}$, $\mathbf{C_2}$, $\mathbf{m_2}$ and $\mathbf{V_2}$. These two types are regarded as occurring one after the other in the loading history.

Two possible sequences of their occurrence will be discussed:

1) At first, all the $\mathbf{N_1}$ cycles of type 1 occur, causing the crack length to change from $\mathbf{l_0}$ to a certain value of $\mathbf{l_{11}}$; these are followed by all the $\mathbf{N_2}$ cycles of type 2, resulting in the crack length change from $\mathbf{l_{11}}$ to $\mathbf{l_{1f}}$;
2) At first, all the $\mathbf{N_2}$ cycles of type 2 occur, causing the crack length to change from $\mathbf{l_0}$ to a certain $\mathbf{l_{21}}$; these are followed by all the $\mathbf{N_1}$ cycles of type 1, resulting in the crack length change from $\mathbf{l_{21}}$ to $\mathbf{l_{2f}}$.

Based on Eq.20, we obtain:

$$\mathbf{N_1 = \int_{l_0}^{l_{11}} \frac{dl}{V_1} = \int_{l_{21}}^{l_{2f}} \frac{dl}{V_1}} \qquad \text{Eq.24}$$

$$\mathbf{N_2 = \int_{l_0}^{l_{21}} \frac{dl}{V_2} = \int_{l_{11}}^{l_{1f}} \frac{dl}{V_2}}, \qquad \text{Eq.25}$$

from which it follows that

$$\mathbf{\int_{l_0}^{l_{21}} \left(\frac{1}{V_2} - \frac{1}{V_1}\right) dl = \int_{l_{11}}^{l_{1f}} \left(\frac{1}{V_2} - \frac{1}{V_1}\right) dl + \int_{l_{2f}}^{l_{1f}} \frac{dl}{V_1}}. \qquad \text{Eq.26}$$

Let us assume that the function $\mathbf{V_2(l)/V_1(l)}$ is constant throughout the range of crack lengths l under consideration. Then, from Eqs. 24-26 it follows that $\mathbf{l_{1f} = l_{2f}}$, i.e. the resultant crack growth is independent of the order of occurrence.

If the function $\mathbf{V_2(l)/V_1(l)}$ is found to be monotonically increasing, then, in view of Eq. 25, we get

$$\int_{l_0}^{l_{2f}} \left(\frac{1}{V_2} - \frac{1}{V_1}\right) dl > \int_{l_{11}}^{l_{1f}} \left(\frac{1}{V_2} - \frac{1}{V_1}\right) dl \qquad \text{Eq.27}$$

and from Eq. 26 it follows that $l_{1f} > l_{2f}$.

Likewise, it is established that the inequality $l_{1f} < l_{2f}$ is true for the monotonically decreasing function $V_2(l)/V_1(l)$.

These three results may be summarized by one conclusion: the maximum crack growth is obtained, if the first type of cycles considered is that with the algebraically minimum value of parameter ω

$$\omega = \frac{dV/dl}{V} = m \cdot \frac{d(\Delta K_{ef})/dl}{\Delta K_{ef}}. \qquad \text{Eq.28}$$

Judging from Eq. 28, priority in analysis should be given to the types of cycles with such loads that lead to high rates of crack growth with its small acceleration (the principle of "quick decelerating crack").

3.2.2. General case of a loading history

It is assumed that loading is produced in cycles of n types with the parameters $(\Delta K_{ef})_i$, N_i, C_i, m_i, V_i, and ω_i, where i = 1, 2, ..., n. Every i-th type of cycles is realized in full (i.e. all the N_i cycles in succession), otherwise the remainder should be treated as a separate type.

Let the sequence of cycles will be established so that each subsequent cycle type will have a greater value of quantity ω_i relative to the previous type at their respective crack lengths. It will be proved that such a design loading sequence results in the greatest possible crack growth.

To this end, we shall resort to the reductio ad absurdum. Let the maximum growth occurs in some other sequence of the same n types of cycles. Then, this new sequence will have such types of cycles i and i+1, for which $\omega_i > \omega_{i+1}$. By changing the order of their occurrence, we have type (i-1) followed by (i+1) and then by i-й. In this case, according to section 3.2.1, the crack increment caused by growth between $l_{(i-1)f}$ and $l_{(i+1)f}$ will be larger than in the original sequence and, hence, the final crack length will increase upon occurrence of the remaining types of cycles. This is contradictory to the original assumption, which proves that the statement in question is true.

The proposed rule for establishing a design history is illustrated by the example of a surface crack in a massive body loaded by cycles of three types, as shown in Fig. 8.

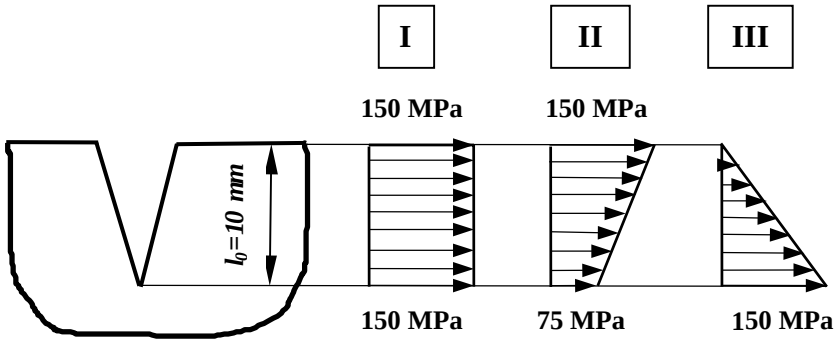

Fig. 8. An example of various crack loading conditions in half-plane

With each type, cyclic tensile stresses vary from 0 to maximum values shown in the stress patterns. The linear laws of maximum load variations were taken to be unchanged with crack growth. The values of ΔK_{ef} were found from the Handbook (1986) for an edge crack in elastic semi-infinite plane.

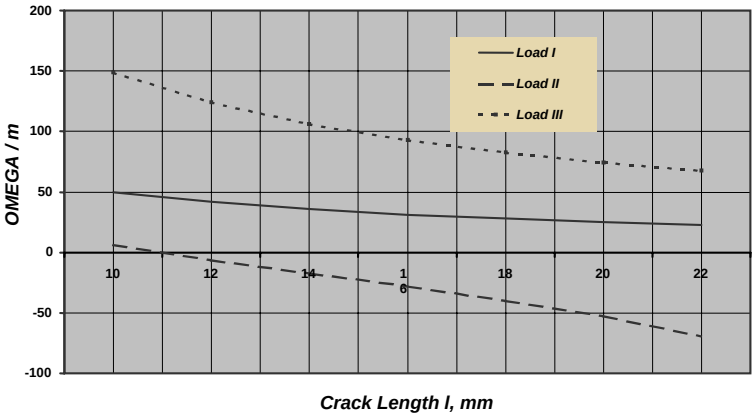

Fig. 9. Variations in ω/m for the crack loading cases of Figure 8

The inequalities $\omega_{II} < \omega_{I} < \omega_{III}$ are true throughout the crack length range under consideration (see Fig. 9). In full accord with the principle of "quick decelerating crack", the greatest total increase in length was found in case 5 of Table 2, with types of cycles coming in order of increasing ω, and the minimum one was observed in case 3, where this order was totally disrupted. It may be easily seen that use of the rain-flow method, shadow method or even of the peak counting method would lead to loading cases 3 or 4 of the Table, but not to the most hazardous case 5.

Some pair wise combinations of the cycle types examined are another testimony to the validity of the proposed principle of establishing a design loading sequence (cases 1 and 5 for types I and II, cases 1 and 4 for types II and III, etc.).

Table 2. Crack length increase for loading cases in Figure 8.

No	Order of Loading	Austenitic Stainless Steel 316LN-IGO ($m = 3.75$; $C = 1.78 \cdot 10^{-12}$) *) $N_I = N_{II} = N_{III} = 4000$	Copper Alloy CuAl25-IGO ($m = 2.76$; $C = 3.52 \cdot 10^{-11}$) *) $N_I = N_{II} = N_{III} = 6000$
		Δl, mm	
1	I + II + III	3.10 + 0.60 + 4.70 = **8.40**	2.97 + 0.87 + 3.96 = **7.80**
2	II + III + I	0.62 + 0.61 + 3.99 = **5.22**	0.92 + 1.10 + 3.88 = **5.90**
3♥)	III + I + II	0.42 + 3.40 + 0.56 = **4.38**	0.73 + 3.30 + 073 = **4.86**
4	I + III + II	3.10 + 2.90 + 0.46 = **6.46**	2.97 + 2.70 + 0.74 = **6.41**
5♣)	II + I + III	0.62 + 3.53 + 7.55 = **11.70**	0.92 + 3.38 + 5.00 = **9.30**
6	III + II + I	0.42 + 0.62 + 3.86 = **4.90**	0.73 + 0.92 + 3.72 = **5.37**

♥) Minimum total crack increment.

♣) Maximum total crack increment.

*) Shown values of m and C of Eq.20 are for crack length measured in meters and SIF – in MPA√m.

3.3. Recommendations for analyses

If calculations are performed to assess the fatigue crack growth under conditions of actual cyclic loading, then, as mentioned above, it is advisable to apply the rain-flow method in establishing the design cycles.

With calculations made for a projected loading sequence, it should be kept in mind that in reality fatigue crack growth is accompanied both by crack tip displacement with change of the adjacent material, and by a certain interplay between cycles of different types. Therefore, the following regulatory procedure for establishing design cycles and crack growth analysis may be proposed aiming at conservative inclusion of the factors discussed in sections 3.1 and 3.2:

a) Divide all cycle types under consideration between segments of predicted crack growth path. Each segment should have the type of cycles with minimum value of ω for any one of crack lengths of this segment.

b) Evaluate SIF variation cycles over predicted crack growth path according to the cycle types

distribution between the segments, as it prescribed in item a).

c) Form design SIF variation cycles by means of the maximum range principle. The shadow method is advised for this purpose.

d) Analyze fatigue crack growth on a basis of the relationships of Eq.20 type using formed design cycles. The design cycles should be used in order of decreasing SIF range.

e) It is possible for some cycle type that during the analysis all recurrences are already analysed, whereas the crack length including calculated increment do not yet achieved higher boundary of the path segment, assigned for this cycle type according to item a). If so, return to item a), re-divide the cycle types taking into account the new calculated boundary of the segment for mentioned cycle type. Then the items b)-d) are to be repeated.

The proposed procedure may be made less conservative by means of dividing the predicted crack growth path into a number of portions. Dimensions of this portions are to be taken from considerations that interaction of the cycle types in fatigue damage cumulation at the crack tip manifests itself within the portions only and there is no the interaction between the cycles of different portions. In such a situation, the maximum range principle of item c) should be applied for each portion of the path separately and only for the SIF cycles acting into this portion.

The proposed procedure is quite complicated and probably may be simplified on a basis of further research of interplay of mentioned Cases 1 and 2. However, even now the procedure is easy for coding and suitable for evaluations performed by computer.

4. CONCLUDING REMARKS

This paper discusses some improved techniques for setting up design stress, strain and SIF cycles.

To allow for plastic effects in a crack-free component, an updated analytical procedure is proposed for describing a true stress-strain curve based on ultimate stress, yield stress and elasticity modulus data. Besides, this approach offers an additional benefit of calculating the value of uniform elongation. Such improved description is applicable both to the projected and to the actual loading history.

It has been noted that in dealing with an actual loading history it is expedient to use the rain-flow method in establishing design cycles of stresses / strains (for a crack-free component) or SIF variations (if growth of an existing crack is assessed).

The rain-flow method would not do for a projected loading history, where it is necessary to consider the most unfavourable load occurrence sequence, as the resulting estimates may be non-conservative. In this case, use of the proposed shadow method ensures fulfilment of the maximum cycle range principle in forming stress / strain cycles for crack-free components.

In setting up SIF variation cycles in a projected loading sequence for a component with a crack, it is suggested that the shadow method should be combined with assessment of parameter ω, which accounts for load distribution over the component (the principle of “quick decelerating crack”).

It should be noted that use of the peak counting method to set up design stress / strain cycles is bound to produce conservative results (in many instances, unduly conservative). In the case of SIF cycles, however, the result may well be non-conservative, as the load distribution over the component (parameter **ω)** is disregarded.

Establishment of SIF cycles according to the planned chronological order of loads appears inappropriate for the following reasons:

- if the planned chronological order is strictly adhered to during operation, it may be viewed as an actual history, in which case it is necessary to make additional use of the rain-flow method to allow for the mutual influence of various cycles;
- if the planned chronological order is disrupted (as is usually the case), then from the viewpoint of standard conservatism it is necessary to consider the worst sequence of load occurrence, which calls for the method of SIF cycle formation proposed in this paper.

On the whole, this paper illustrates the basic distinctions between the methods of establishing design stress, strain and SIF cycles for analysing the ***current condition*** of a component (the case of an actually occurred history) and those involved in assessing its ***residual lifetime*** or ***life extension*** (the case of a projected history).

REFERENCES

[1] ASME, (2001), “ASME Boiler & Pressure Vessel Code”, ASME, N.Y.

[2] Birger, I. A., Mavlyutov, R. R., (1986), “Strength of Materials”, Nauka, Moscow (in Russian)..

[3] Guidelines, (2004), RD EO 0330-01, «Guidelines for Strength Analysis During Operation of Equipment and Pipelines of RBMK, WWER and EGP Reactor Facilities”, ENES-RDIPE, Moscow

[4] Handbook, (1986), “Stress Intensity Factors Handbook”, Editor-in-chief Y. Murakami, v.1, Pergamon Press, Oxford-New York-Beijing-Frankfurt-Sâo Paulo-Sydney-Tokyo-Toronto.

[5] Kuzema, I. D., (1975), Zavodskaya Laboratorya, No.12, p. 32 (in Russian).

[6] Makhutov, N. A., (1981), “Deformation Criteria of Fracture and Strength Analysis of Structure Components”, Mashinostroenie, Moscow.

[7] Matsuishi, M., Endo, T., (1968), Jrnl. of the Japanese Society for Mechanical Engineers, v.71, March (in Japanese).

[8] Regulations, (1989), PNAE G-7-002-86, “Regulations for Strength Analysis of Nuclear Power Plant Equipment and Pipelines”, Energoatomizdat, Moscow (in Russian).

[9] RCC-M, (1988), “Design and Construction Rules for Mechanical Components of PWR Nuclear Islands”, AFCEN, Paris (Translated from the French).

[10] RCC-MR, (2002), “Design and Construction Rules for Mechanical Components for FBR Nuclear Islands”, AFSEN, Paris (Translated from French).

[11] Shevandin, E.M., Razov, I. A., (1965), “Cold Brittleness and Ultimate Plasticity of Shipbuilding Metals”, Sudostroenie, Leningrad.

[12] Tashkinov, A.V., (1998), Nuclear Engineering and Design, v. 179, pp. 101-107.

[13] Tashkinov, A.V. (1999), Trans. of the 15th Int. Conf. on Structural Mechanics in Reactor Technology (SMiRT 15), V-161.

